Article

Antitumor Effects of Afatinib on Tumorigenic Potentials in Triple Negative Breast Cancer

Deok-Soo Son [1,*], Tamara J. Martin [1], Rosa Mistica C. Ignacio [1], Sydney E. Harville [2], Eun-Sook Lee [3], and Samuel E. Adunyah [1]

[1] Department of Biochemistry, Cancer Biology, Neuroscience and Pharmacology, School of Medicine, Meharry Medical College, Nashville, TN 37208, USA
[2] Biology Program, Savannah State University, Savannah, GA 31404, USA
[3] Department of Pharmaceutical Sciences, College of Pharmacy, Florida A&M University, Tallahassee, FL 32301, USA
* Correspondence: dson@mmc.edu
Received: 28 December 2025; Revised: 27 March 2026; Accepted: 8 May 2026; Published: 19 May 2026

Abstract: Triple-negative breast cancer (TNBC), a highly aggressive subtype characterized by frequent relapse, metastasis, and poor prognosis, exhibits elevated epidermal growth factor receptor (EGFR) expression. Our prior research demonstrated that afatinib, a tyrosine kinase inhibitor, effectively suppressed EGFR-mediated downstream, including AKT and ERK, and reduced epithelial-to-mesenchymal transition (EMT) markers in human TNBC cell models. This study was designed to extend afatinib's efficacy in mitigating tumorigenic potentials in murine TNBC models. We employed cell viability assays, signaling pathway analyses, cytokine profiling, cell cycle-related protein assessments, and diet-induced obese mouse models to elucidate afatinib's therapeutic benefits. Afatinib exhibited superior inhibition on cell viability in murine TNBC cells compared to erlotinib, gefitinib, and lapatinib. In PY8119 TNBC cells, afatinib inhibited AKT and ERK phosphorylation, downregulated vimentin and N-cadherin expression, and suppressed cell migration and invasion. Additionally, afatinib reduced proinflammatory chemokine levels, disrupted cell cycle progression, and upregulated necrosis-associated proteins. In diet-induced obese mouse models, afatinib significantly reduced tumor burden. Collectively, these findings suggest that afatinib attenuates TNBC tumorigenicity by inhibiting EGFR-mediated downstream signaling and EMT markers, downregulating proinflammatory chemokines, and disrupting cell cycle progression, supporting its potential as a therapeutic agent for TNBC at preclinical evaluation.

Keywords: afatinib; chemokine; EGFR; triple negative breast cancer

1. Introduction

Triple-negative breast cancer (TNBC) accounts for approximately 15–20% of all breast malignancies and represents a clinically aggressive entity with frequent metastasis and high disease-related mortality [1]. This subtype is defined by the lack of estrogen receptor, progesterone receptor, and human epidermal growth factor receptor 2 (HER2) expression, which severely limits available targeted treatment options and contributes to unfavorable patient outcomes [1]. At the molecular level, TNBC consists of multiple biologically diverse subgroups, including basal-like, immunomodulatory, mesenchymal-like, and luminal androgen receptor phenotypes [2]. Such heterogeneity complicates therapeutic development and underlines the urgent need for effective subtype-informed therapeutic strategies. Relative to hormone receptor–positive breast cancers, TNBC exhibits increased expression levels of epidermal growth factor receptor (EGFR) and enhanced production of proinflammatory chemokines [3]. EGFR-driven signaling pathways have been involved in the regulation of these chemokines, potentially intensifying inflammatory conditions within the tumor microenvironment and promoting tumor aggressiveness [4]. These observations suggest that pharmacologic inhibition of EGFR using tyrosine kinase inhibitors (TKIs) may offer a rational therapeutic approach for TNBC. However, EGFR-targeted treatments have shown limited efficacy in TNBC, in part due to atypical EGFR localization—particularly nuclear EGFR—which is frequently observed in this subtype and contributes to therapeutic resistance [5]. The complexity of EGFR-associated signaling networks across TNBC subtypes further complicates clinical responses, highlighting the necessity for alternative or optimized therapeutic strategies to overcome drug resistance [6].

Among EGFR-targeted TKIs, comparative analyses in basal-like and mesenchymal-like TNBC cell models have demonstrated that afatinib exerts greater antiproliferative activity than lapatinib, gefitinib, or erlotinib [7]. Afatinib effectively attenuates AKT and ERK signaling in both TNBC subtypes and selectively suppresses mesenchymal markers, including N-cadherin and vimentin, in mesenchymal-like TNBC cells [7]. Nevertheless, afatinib has been shown to differentially regulate cytokine- and oncology-related signaling pathways across TNBC subtypes, suggesting that tumor heterogeneity may influence therapeutic responsiveness [7]. The tumor microenvironment plays a critical role in driving TNBC growth and metastasis [8]. Our previous *in vitro* study was limited by only the use of cell culture models [7], not to recapitulate the complex tumor microenvironment. Therefore, rigorous *in vivo* validation is essential to evaluate the therapeutic potential of afatinib against TNBC progression.

To address this limitation, the present study was designed to evaluate the antitumor efficacy of afatinib in clinically relevant preclinical TNBC mouse models. Although immunodeficient xenograft models are commonly used for human TNBC cells, they lack functional adaptive immunity (particularly T and B cells) and thus cannot accurately reflect the intact tumor immune microenvironment. Given that obesity is associated with worse overall survival in TNBC patients and has been shown to accelerate tumor progression in experimental models [9], we employed a diet-induced obesity model in immunocompetent mice. Orthotopic implantation of murine TNBC cells into the mammary fat pad was used to evaluate afatinib's therapeutic efficacy in a physiologically relevant setting that preserves an intact tumor immune microenvironment. We selected murine TNBC models representing the basal-like and mesenchymal subtypes of human TNBC. Building upon our prior in vitro findings in human TNBC cells [7], including assessments of cell viability, EGFR-mediated signaling, epithelial-to-mesenchymal transition (EMT) markers, and cytokine profiles, this study further investigated functional cellular behaviors (migration and invasion), cell cycle progression and associated gene expressions, as well as *in vivo* tumor progression using bioluminescence imaging for tumor tracking in TNBC orthotopic mouse models reflecting the intact tumor immune microenvironment.

2. Materials and Methods

2.1. Mouse TNBC Cell Lines and Culture

Murine TNBC cell lines representing mesenchymal-like (PY8119) and basal-like (PY230) subtypes [10] were obtained from the American Type Culture Collection (ATCC; Manassas, VA, USA). To ensure culture integrity, cells were routinely evaluated for mycoplasma contamination using the MycoAlert Detection Kit (Lonza, Allendale, NJ, USA), and all tests confirmed the absence of contamination. Cells (passage number < 20) were cultured in Roswell Park Memorial Institute 1640 (RPMI 1640) medium supplemented with 10% fetal bovine serum (FBS), 1% penicillin–streptomycin, and maintained at 37 °C in a humidified incubator containing 5% CO_2. All cell culture reagents and supplements were purchased from Invitrogen (Grand Island, NY, USA). The TKIs used in this study (afatinib, lapatinib, gefitinib, and erlotinib) were obtained from Cayman Chemical (Ann Arbor, MI, USA).

2.2. Cell Viability Assay

The MTT assay was conducted for cell viability, which relies on the mitochondrial reduction of 3-(4,5-dimethylthiazol-2-yl)-2,5-diphenyltetrazolium bromide to purple formazan crystals, as outlined in prior work [9]. In brief, cells were plated into 24-well dishes and allowed to grow for 48 h in a humidified incubator at 37 °C with 5% CO_2. The medium was then aspirated, and cells were washed twice using PBS (pH 7.4) to eliminate any traces of serum or debris. Next, 1 mg/mL MTT prepared in phenol red-free medium mixed with PBS (4:1 ratio) was introduced to the wells, followed by a 3-h incubation period in the dark at 37 °C. After discarding the MTT reagent, 500 µL of isopropanol was dispensed per well to solubilize the intracellular formazan. The plates were placed on a shaker for 10 min at ambient temperature until the crystals fully dissolved, with visual inspection confirming no residual precipitates. Absorbance readings were recorded at 595 nm on a Bio-Rad microplate reader (Hercules, CA, USA). Data were expressed as percentages relative to the vehicle-treated control wells to quantify viability changes.

2.3. Western Blot Analysis

Total cellular proteins were extracted, separated by SDS–polyacrylamide gel electrophoresis (SDS-PAGE), and electrotransferred onto nitrocellulose membranes as described previously [9]. Membranes were probed with antibodies recognizing AKT, ERK, SAPK/JNK, p38, their corresponding phosphorylated species, and epithelial–mesenchymal transition markers including E-cadherin, N-cadherin, and vimentin (Cell Signaling Technology, Beverly, MA, USA). β-Actin (TU-02; Santa Cruz Biotechnology, Dallas, TX, USA) served as an internal loading reference. Immunoreactive signals were detected using enhanced chemiluminescence reagents (MilliporeSigma,

St. Louis, MO, USA), and band intensities were quantified by densitometric analysis with ImageJ software (v1.54P; National Institutes of Health, Bethesda, MD, USA; https://imagej.net (accessed on 23 July 2023))

2.4. Migration and Invasion Assay

For Transwell-based motility assays, cells were prepared at a density of 2×10^5 cells/mL in serum-free RPMI-1640 supplemented with 0.5% bovine serum albumin. Cell migration was assessed using uncoated 24-well Transwell inserts (Greiner Bio-One), whereas invasion assays were conducted using inserts pre-coated with Matrigel (BD Biosciences; diluted 1:3 in PBS). Cells were exposed to afatinib at the IC50 concentration and maintained under these conditions overnight. Following incubation, non-migratory cells were removed, and cells that traversed the membrane were fixed in 3.7% formaldehyde and subsequently stained with 0.1% crystal violet. Excess stains were eliminated by PBS washes. Migrated or invaded cells were visualized by light microscopy at 400× magnification and quantified from three randomly selected microscopic fields.

2.5. Proteomic Array Analysis

Cytokine-associated protein expression patterns were analyzed using the Proteome Profiler Mouse XL Cytokine Array (ARY028; R&D Systems, Minneapolis, MN, USA) in accordance with the manufacturer's recommended procedures and our previously published methodology [9]. Membrane spot signals were captured and quantified using ImageJ software (https://imagej.net). For data processing, background signals were subtracted, and data were normalized to internal reference spots to ensure consistent quantification across samples.

2.6. Fluorescence-Activated Cell Sorting Analysis

Cells were seeded at uniform density and cultured for 24 h. Subsequently, cells were treated in triplicate with afatinib or media alone (control) for 24 or 48 h. Both adherent and non-adherent cells were collected using cold PBS and stained overnight with propidium iodide (50 mg/mL in 0.1% *w*/*v* sodium citrate, 0.1% *v*/*v* Triton X-100). Following incubation, samples were analyzed via a FACScan flow cytometry (BD Biosciences), and the proportions of cells in G0/G1, S, and G2/M phases were quantified using FloJo software (Tree Star Inc., Ashland, OR). Data were expressed as percentages relative to untreated control cells.

2.7. Polymerase Chain Reaction (PCR) Array

Cell cycle–associated transcriptional changes were examined using the RT^2 Profiler^{TM} Mouse Cell Cycle PCR Array (330231; Qiagen, Frederick, MD, USA) in accordance with procedures established in our previous study [11]. Total RNA was isolated from TNBC cells with elimination of residual genomic DNA. Complementary DNA synthesis was carried out at 42 °C for 15 min, followed by heat-mediated termination of reverse transcriptase activity at 94 °C for 5 min. Quantitative PCR amplification was performed on a Bio-Rad CFX96 Touch Real-Time PCR platform (Hercules, CA, USA) using reagents and protocols provided by the manufacturer. Thermal cycling included an initial denaturation step at 95 °C for 10 min and 40 subsequent amplification cycles consisting of 95 °C for 15 s and 60 °C for 60 s. Gene expression data were processed and interpreted using the GeneGlobe Data Analysis Center (Qiagen; https://geneglobe.qiagen.com/us/analyze/ (accessed on 24 July 2025)) according to the recommended analysis pipeline.

2.8. Diet-Induced Obese Mouse and Orthotopic Mammary Fat Pad Models

All animal experiments were conducted in accordance with protocols approved by the Institutional Animal Care and Use Committee of Meharry Medical College (eProtocol #16-03-511) and adhered to the National Institutes of Health Guide for the Care and Use of Laboratory Animals. Female C57BL/6J mice (4 weeks old) were purchased from Jackson Laboratory (Bar Harbor, ME, USA) and maintained in a specific pathogen–free environment under controlled conditions (22 ± 2 °C, 40–60% humidity, and a 12-h light/dark cycle). Diet-induced obesity was established by providing mice with a high-fat diet (D12492; 60% kcal from fat; Research Diets Inc., New Brunswick, NJ, USA) for a duration of 9 weeks, as described previously [9]. For orthotopic tumor implantation, PY8119Luc TNBC cells (3×10^6 cells per mouse) were resuspended in a 1:1 mixture of PBS and Matrigel and injected into the right fourth mammary fat pad. Beginning one week after tumor inoculation, mice received afatinib at a dose of 10 mg/kg by oral gavage, formulated in 0.5% (*w*/*v*) methylcellulose, five times per week for four consecutive weeks. Tumor progression was assessed weekly using bioluminescence imaging. Prior to imaging, mice were anesthetized with 3% isoflurane and administered D-luciferin intraperitoneally (125 mg/kg; Cayman Chemical, Ann Arbor, MI, USA). Imaging was initiated 5 min after luciferin injection using the In-Vivo

MS FX PRO optical imaging system (Carestream, NY, USA), with photon emission captured over a 1-min interval. Quantitative analysis of luminescent signals within defined regions of interest was performed using Molecular Imaging software (Carestream). In parallel, tumor size was evaluated weekly by caliper measurements, and volumes were calculated using the formula: (length × width^2)/2.

2.9. Statistical Analysis

Results are expressed as the mean ± standard deviation (SD). Differences were considered statistically significant at $p < 0.05$. Pairwise comparisons between two groups were performed using Student's *t*-test. Comparisons involving more than two groups were analyzed by one-way analysis of variance (ANOVA) followed by Tukey's post-hoc test for significant findings.

3. Results

3.1. Afatinib Exhibits Superior Cytotoxicity in Mesenchymal and Basal-Like TNBC Cells

The cytotoxicity of four TKIs (erlotinib, gefitinib, lapatinib, and afatinib) was examined in murine TNBC cell lines representing mesenchymal-like (PY8119) and basal-like (PY230) subtypes. Cell viability was measured via MTT assay, yielding the following IC50 values: 50.0 μM (erlotinib), 20.4 μM (gefitinib), 6.8 μM (lapatinib), and 3.3 μM (afatinib) in PY8119 cells; 50.4 μM (erlotinib), 22.1 μM (gefitinib), 3.13 μM (lapatinib), and 1.93 μM (afatinib) in PY230 cells (Figure 1). In both lines, the rank order of potency remained consistent: afatinib > lapatinib > gefitinib > erlotinib. Afatinib exhibited the strongest inhibitory activity, achieving half-maximal inhibition at substantially lower doses than the other agents. Erlotinib and gefitinib displayed comparable efficacy in the two cell lines, whereas lapatinib and afatinib were markedly more potent in PY230 cells compared to PY8119 cells (Figure 1).

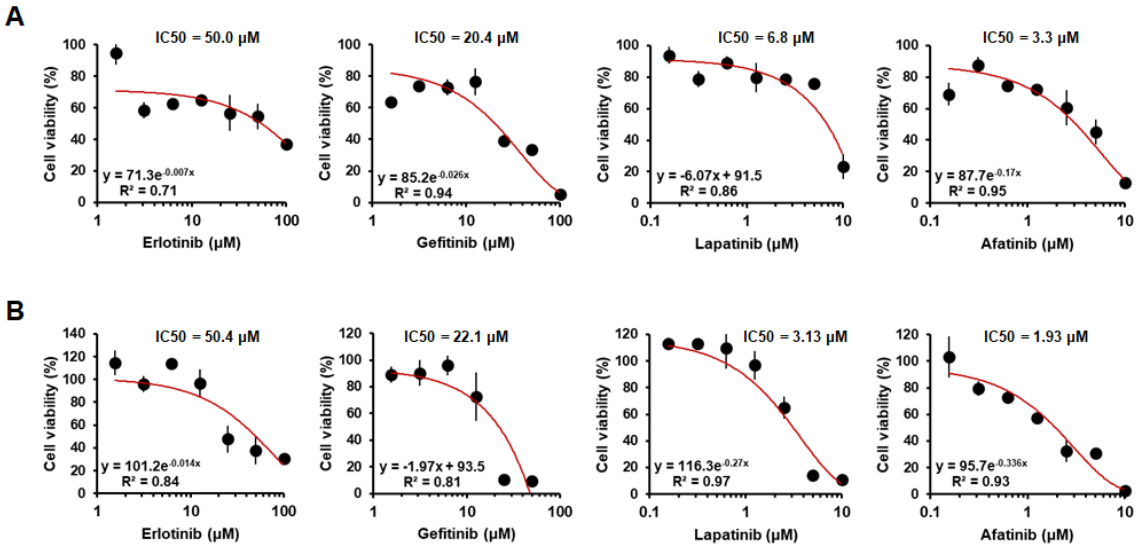

Figure 1. Comparisons of IC50 values for tyrosine kinase inhibitors in mouse mesenchymal-like PY8119 and basal-like PY230 TNBC cells. Comparison of the effects of erlotinib, gefitinib, lapatinib, and afatinib on cell viability in mesenchymal-like PY8119 TNBC cells (**A**) and basal-like PY230 TNBC cells (**B**). Cells were treated with various concentrations of each TKIs for 48 h. Data points represent mean values with vertical bars indicating SD (n = 3). Red trendlines were fitted using exponential, linear, and logarithmic regression models, with the best-fir model selected based on the highest R^2 values (calculated with Microsoft Excel's Data Analysis Toolpak).

3.2. Afatinib Suppresses AKT and ERK Activation, EMT Markers, Cell Migration, and Invasion

Given the superior cytotoxicity of afatinib among the tested TKIs (Figure 1), this agent was chosen for further investigation of its impact on intracellular signaling in PY8119 and PY230 cells. Treatment with afatinib markedly suppressed phosphorylation of AKT and ERK in both cell lines, without appreciably altering SAPK/JNK or p38 MAPK activation (Figure 2A). In mesenchymal-like PY8119 cells, afatinib also reduced expression of the EMT markers vimentin and N-cadherin (Figure 2B) with lack of E-cadherin expression (data not shown). In contrast, no appreciable alteration in E-cadherin levels was detected in basal-like PY230 cells (Figure 2B) with lack of N-

cadherin expression (data not shown). Using PY8119 cells, we further evaluated functional effects on motility. Afatinib treatment substantially inhibited both cell migration and invasion relative to vehicle-treated controls (Figure 2C,D).

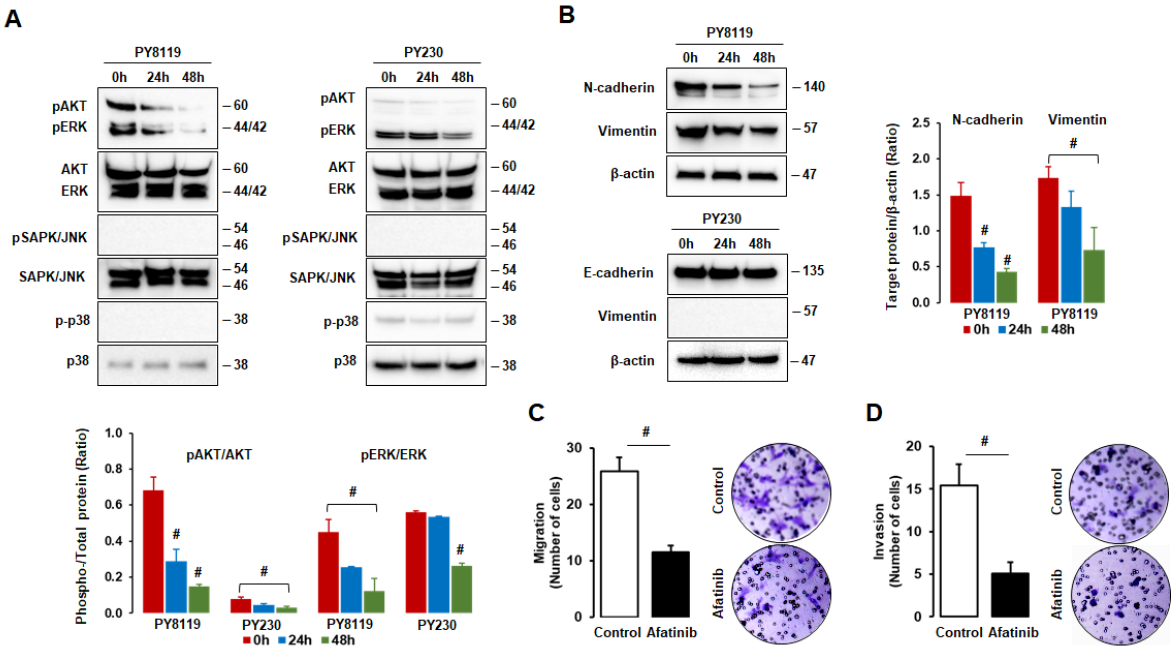

Figure 2. Afatinib-regulated signaling pathways and cell migration and invasion in TNBC cells. (**A**) Effects of afatinib on the phosphorylation of AKT, ERK, SAPK/JNK, and p38 in PY8119 and PY230 cells. (**B**) Effects of afatinib on EMT-associated proteins (vimentin, N-cadherin, and E-cadherin) in PY8119 and PY230 cells. Cells were treated with afatinib at its IC50 concentration for 24 and 48 h. β-actin served as a loading control. (**C**) Effects of afatinib on cell migration in PY8119 cells. (**D**) Effects of afatinib on cell invasion in PY8119 cells. Cells were treated with afatinib at its IC50 concentration overnight. # indicates statistical significance ($p < 0.05$, n = 3) between groups, as determined by one-way ANOVA with Tukey's pairwise comparisons or Student's *t*-test.

3.3. Afatinib Downregulates Proinflammatory Chemokines in Both Mesenchymal-like and Basal-like TNBC Cells

Human basal-like and mesenchymal-like TNBC cells highly express the proinflammatory chemokines CXCL1 and CXCL8 [3]. To determine whether PY8119 and PY230 cells recapitulate the cytokine profile of human TNBC cells and to evaluate the effect of afatinib on these cytokines, we investigated cytokine profiles. Both PY8119 and PY230 cells showed high expression of CXCL1 (Figure 3), reflecting the chemokine profile of human TNBC cells. In PY8119 cells, afatinib reduced CXCL1 and CX3CL1 protein levels at 24 and 48 h, and PAI-1 levels at 48 h (Figure 3, left panel). In PY230 cells, afatinib decreased CX3CL1 and CXCL1 protein levels at 24 and 48 h, respectively (Figure 3, right panel). Furthermore, afatinib reduced CXCL5 and IGFBP5 protein levels at 24 and 48 h (Figure 3).

3.4. Afatinib Disrupts Cell Cycles by Modulating Cell Cycle-Related Genes in PY8119 TNBC Cells

PY8119 cells were selected for subsequent experiments because they are highly aggressive *in vivo*, forming palpable tumors as early as day 5, whereas PY230 cells are more differentiated and display markedly slower growth, with palpable tumors appearing only after more than 20 days [10]. Because afatinib attenuated EGFR downstream significantly AKT and ERK activation (Figure 2A), which are related to cell growth, we further assessed if afatinib modifies cell cycles using PY8119 cells. Cell cycle analysis revealed that afatinib did not affect critically sub-G1 phase (Figure 4A), which indicates apoptotic cell portion. Afatinib increased G1 phase at 24 h, with increased S phase and decreased G2 phase at 48 h (Figure 4A). Continuedly, we assessed afatinib-induced cell cycle-related genes using human cell cycle PCR array (Figure 4B). Afatinib upregulated GADD45A, ATR, RB1, DDIT3, PMP22, and CDKN1B, and downregulated CDKN3, CCND1, CDC25C, MKI67, CDC20, CCNB1, CCNA2, BIRC5, and CCNB2 (Figure 4C). Although afatinib modified CDKN1A, AURKA, CDC6, NEK2, and AURKB, these are low expression genes in PY8119 cells (Figure 4C).

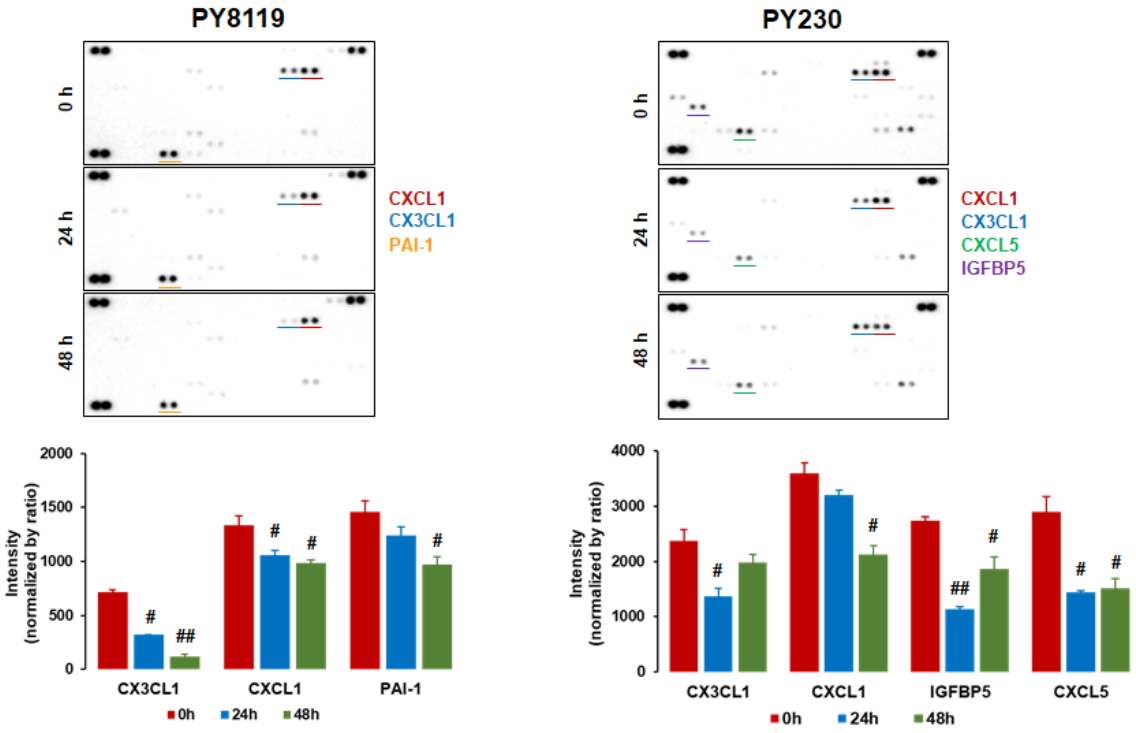

Figure 3. Effects of afatinib on cytokine profiles in PY8119 and PY230 TNBC cells. Cells were treated with afatinib at their respective IC50 concentration for 24 and 48 h. Cytokine expression levels were quantified, revealing significant changes. Statistical significance was determined by one-way ANOVA followed by Tukey's post-hoc test. (# and ## indicate $p < 0.05$; n = 2 biological duplicates) for comparisons between groups. PAI-1, plasminogen activator inhibitor-1; IGFBP5, insulin-like growth factor binding protein 5. See Supplementary Materials S1 for the full list of cytokines measured.

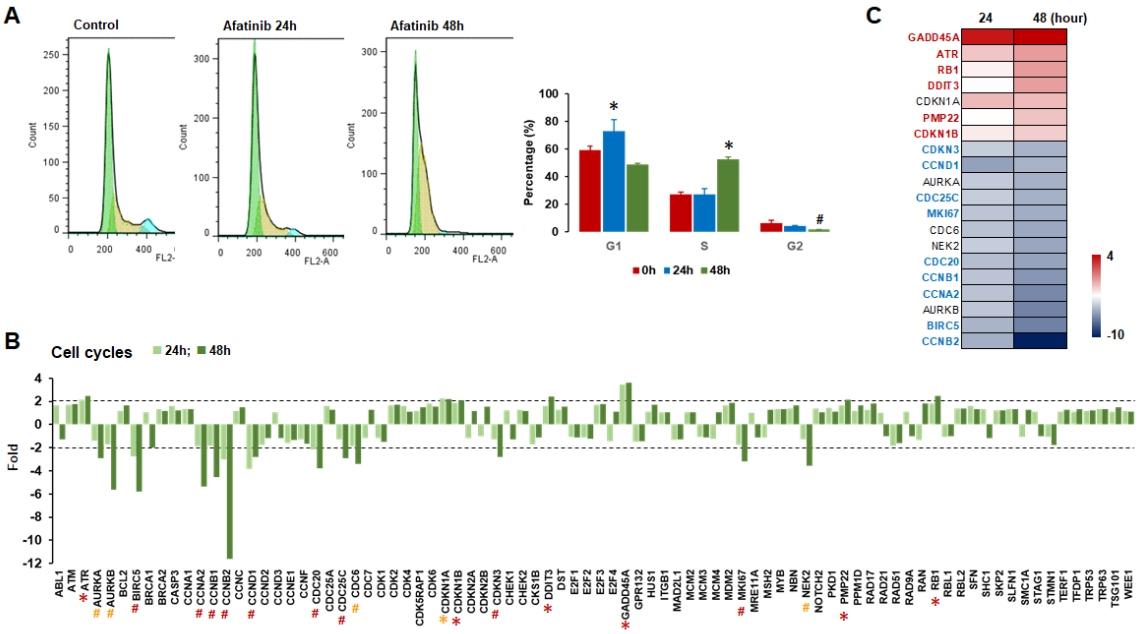

Figure 4. Effects of afatinib on cell cycle distribution and cell cycle-related gene expression in PY8119 TNBC cells. (**A**) Effect of afatinib on cell cycle progression in PY8119 cells. Cells were treated with afatinib at its IC50 concentrations (3.3 μM) for 24 or 48 h. The percentage of cells in each phase of the cell cycle was determined by flow cytometry. Statistical significance was determined by one-way ANOVA followed by Tukey's post-hoc test (* and # indicate $p < 0.05$, n = 3) for comparisons between groups. (**B**) Effects of afatinib on cell cycle-related genes in PY8119 cells assessed by a human cell cycle PCR array. Total RNA was collected at 0, 24, and 48 h after afatinib treatment for a time-course study. Dotted lines indicates a 2-fold increase or decrease in expression. Genes

showing >2-fold change were considered afatinib-regulated genes. Red * and # indicate >2-fold upregulation and downregulation, respectively. Yellow * and # indicate >2-fold changes of low expression genes (average threshold cycle >30 in either control or afatinib-treated samples). Fold-change ($2^{-\Delta\Delta Ct}$) represents the normalized gene expression ($2^{-\Delta Ct}$) in the afatinib-treated sample divided by that in the control. ΔCt is the difference between the cycle threshold (Ct) value of the gene of interest and the reference gene. ΔΔCt is the difference between the ΔCt of the afatinib-treated sample and the ΔCt of the control sample. See Supplementary Materials S2 for gene annotations. (**C**) Heatmap of afatinib-regulated genes following analysis of human cell cycle PCR array. Red and blue letters indicate afatinib-induced up- and down-regulation (fold change), respectively. Black letters indicate low expression genes despite afatinib-induced genes.

3.5. Afatinib Diminishes TNBC Progression Intesified by Diet-induced Obese Mouse Model

Obesity led to poorer overall survival in TNBC patients [9], ob/ob female mice show the greater tumor burden of TNBC compared to wild-type mice [12], and further diet-induced obesity intensified TNBC progression [9]. We used a diet-induced obese mouse model to explore if afatinib diminishes tumor burden intensified by obesity. The body weight gain was confirmed, PY8119Luc cells were injected, afatinib was given by gavage for 4 weeks (Figure 5A). Afatinib treatment reduced the body weight gain compared to control (Figure 5A). We generated luciferase-expressing PY8119Luc cells from parental PY8119 TNBC cells to monitor the tumor burden imaging. Bioluminescence imaging showed that afatinib-treated mice exhibited lower bioluminescence intensity compared to control mice (Figure 5B). Consistent with these findings, afatinib-treated mice displayed reduced tumor volume and weight compared to the control group (Figure 5C,D).

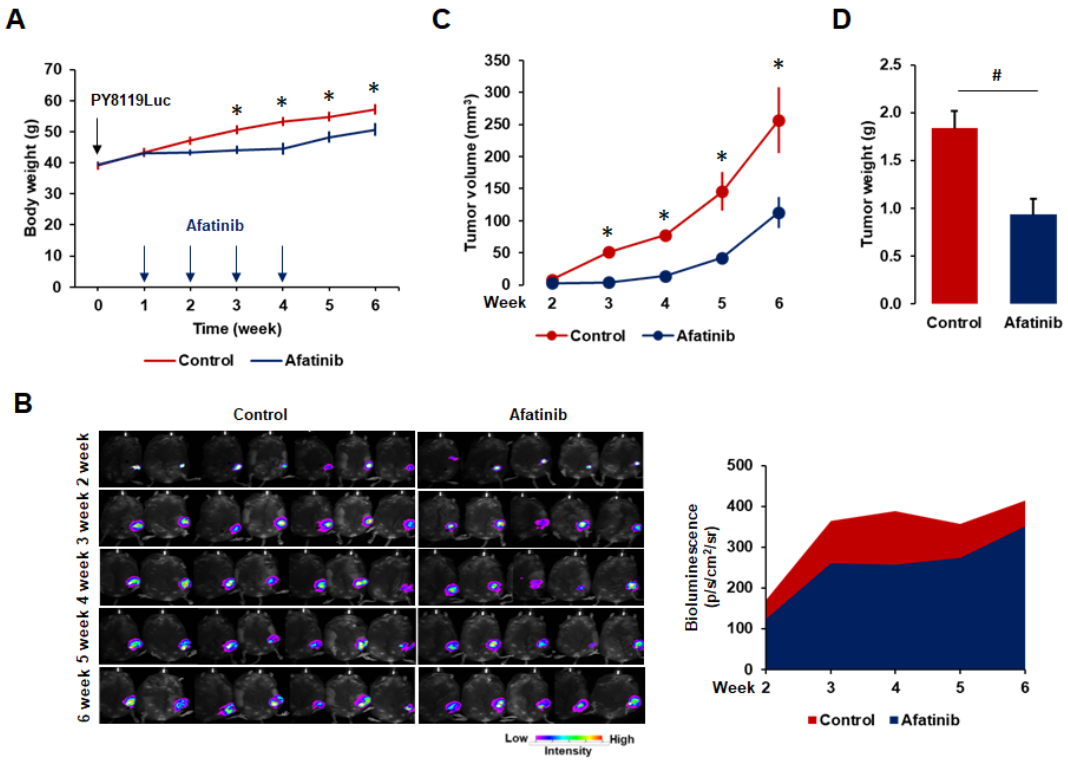

Figure 5. Inhibitory effects of afatinib on the progression of PY8119Luc TNBC cells in diet-induced obese mice using an orthotopic mammary fat pad model. (**A**) Body weights of mice in the control (n = 7) and afatinib-treated (n = 5) groups. (**B**) Bioluminescence images and quantification of tumor burden in PY8119Luc cell-bearing control and afatinib-treated mice. (**C**) Tumor volume over time in control and afatinib-treated mice. (**D**) Tumor weights at the experimental endpoint in control and afatinib-treated mice. Data are expressed as the mean ± SD. * and # indicate statistical significance ($p < 0.05$), as determined by Student's *t*-test.

4. Discussion

This study demonstrated antitumor effects of afatinib in attenuating tumorigenic potential in TNBC using murine TNBC models. Afatinib exhibited superior inhibition on cell viability compared to other TKIs in mouse PY8119 and PY230 TNBC cell lines (Figure 1), corroborating prior findings using human BT549 and MDA-MB-

468 TNBC cells [7]. Notably, afatinib significantly reduced AKT and ERK activation in both murine TNBC cell lines (Figure 2A), consistent with observations in human TNBC cells [7]. Furthermore, afatinib downregulated the expression of N-cadherin and vimentin, key EMT markers, in mesenchymal-like PY8119 cells (Figure 2B), mirroring results in human mesenchymal-like BT549 cells [7]. These findings suggest that PY8119 and PY230 cells reflect human mesenchymal-like and basal-like TNBC subtypes, respectively. Additionally, afatinib suppressed cell migration and invasion in PY8119 cells (Figure 2C,D), aligning with the observed reduction in N-cadherin and vimentin expression (Figure 2B).

The TGFα-EGFR-Akt signaling axis enhances the expression of proinflammatory chemokines in TNBC cells [3]. Proinflammatory chemokines, including CXCL1, CXCL5, and CX3CL1, promote tumor growth and metastasis by fostering an inflammatory tumor microenvironment [13,14]. Afatinib treatment significantly reduced the expression of CXCL1 and CX3CL1 (Figure 3), likely contributing to reducing the inflammatory burden and inhibiting tumor progression. Additionally, afatinib downregulated PAI-1 in PY8119 cells (Figure 3). Given that PAI-1 enhances TNBC cell proliferation, migration, invasion, and tumor growth [15], its reduction by afatinib may attenuate the aggressive behavior of mesenchymal-like TNBC. IGFBP5 exerts context-dependent effects in breast cancer. In MCF-7 cells, IGFBP5 promotes cell adhesion and survival while inhibiting migration and spheroid formation [16,17], indicating dual roles of IGFBP5 as a tumor suppressor or promoter [18]. However, afatinib reduced IGFBP5 expression in basal-like PY230 cells (Figure 3), and the specific role of IGFBP5 in TNBC remains poorly understood, warranting further investigation. Similarly, CXCL5 is known to drive breast cancer cell proliferation and bone colonization [14]. The afatinib-induced reduction of CXCL5 in PY230 cells (Figure 3) may therefore attenuate the progression of basal-like TNBC by limiting these processes.

Afatinib treatment significantly upregulated GADD45A, ATR, RB1, DDIT3, PMP22, and CDKN1B in PY8119 cells (Figure 4B,C). As a stress sensor, GADD45A induces cell cycle arrest [19]. Similar to thymoquinone-induced GADD45A upregulation in MDA-MB-231 cells, which causes cell cycle arrest and cytotoxicity [20], afatinib-induced GADD45A likely contributes to cell cycle disruption and cytotoxic effects in TNBC. ATR, a key mediator of DNA damage-induced cell cycle arrest [21], when upregulated by afatinib may may disrupt progression and enhance chemotherapy sensitivity, consistent with the therapeutic potential of ATR pathway modulation in TNBC [22,23]. RB1 regulates the G1/S transition [24]; its afatinib-induced upregulation may increase S-phase accumulation and contribute to cell cycle disruption (Figure 4A), despite variable RB1 status in TNBC [25]. DDIT3 (CHOP) induces G1 arrest [26] and suppresses tumor growth via AKT/mTOR inhibition [27,28]; afatinib-induced DDIT3 likely enhances G1 arrest and cytotoxicity. PMP22 regulates cell cycle, adhesion, and migration [29]; its upregulation (opposite to pro-proliferative effects of PMP22 knockdown in TNBC [30]) may inhibit proliferation, though its precise role in TNBC cell cycle remains unclear. CDKN1B (p27/KIP1), a key cell cycle inhibitor [31], when induced by afatinib likely promotes arrest and cell death, as seen with FOXE3 knockdown in TNBC [32]. Collectively, afatinib-induced upregulation of these genes synergizes to disrupt cell cycle progression and enhance cytotoxicity in TNBC.

Afatinib significantly downregulated CDKN3, CCND1, CDC25C, MKI67, CDC20, CCNB1, CCNA2, BIRC5, and CCNB2 in TNBC cells (Figure 4B,C). CDKN3 regulates G2/M transition; its downregulation may suppress G2 progression and proliferation [33]. CCND1 (cyclin D1) drives G1/S transition; its downregulation inhibits proliferation, invasion, and colony formation while increasing S-phase accumulation [34]. CDC25C promotes G2/M entry; its suppression may impair progression and viability, similar to G2 arrest via CDC25C-Cyclin B1/CDC2 inhibition [35]. MKI67, a proliferation marker in G2/M [36], downregulation correlates with reduced G2 progression and viability (Figures 1 and 4A). CDC20 is critical for mitotic progression; its downregulation disrupts mitosis and inhibits migration/metastasis [37]. CCNB1 and CCNA2, overexpressed in TNBC with poor prognosis [38–41], when downregulated reduce G2 progression and increase S-phase accumulation (Figure 4A). BIRC5 (survivin) promotes chemotherapy resistance [42]; its downregulation may enhance chemosensitivity and reduce colony formation [43]. CCNB2 drives G2/M and proliferation with poor prognosis [44–46]; its downregulation reduces G2 progression and induces cytotoxicity. Overall, afatinib's downregulation of these genes disrupts key cell cycle transitions, inhibits proliferation and metastasis, and highlights its potential as a targeted TNBC therapy.

Afatinib also modulated additional regulators in PY8119 cells by upregulating CDKN1A (p21, a cell cycle inhibitor [47]) while downregulating AURKA, AURKB, CDC6, and NEK2 (Figure 4C). AURKA/B facilitate G2/M transition and contribute to paclitaxel resistance in TNBC [48,49]; their inhibition suppresses metastasis and colony formation [50,51]. CDC6 aids G1/S transition and serves as a prognostic marker [52–54]. NEK2, an oncogenic kinase overexpressed in TNBC, promotes proliferation and migration [55–57]. Despite low baseline expression of some genes, afatinib's regulation of these genes likely disrupts cell cycle dynamics, suppresses viability, and inhibits migration, attenuating TNBC tumorigenicity.

Diet-induced obesity promotes TNBC progression, whereas intermittent fasting attenuated this effect [9]. Using a diet-induced obese mouse model, this study demonstrated that afatinib significantly reduces TNBC tumor burden (Figure 5). Notably, afatinib treatment led to reduced body weight (Figure 5A). Weight loss is recognized as a potential side effect of afatinib, which has a predictable and manageable side effect profile in advanced non-small cell lung cancer [58,59]. As afatinib-treated mice exhibited no clinical signs of distress compared to controls, afatinib appears to be well-tolerated in this TNBC mouse model.

Clinical trials of EGFR inhibitors in breast cancer have generally shown limited response rates [60]. Overexpression of insulin-like growth factor binding protein 2 (IGFBP2) has been associated with afatinib resistance in TNBC cells [61], suggesting a potential resistance mechanism in TNBC patients. In contrast, TNBC patients with DAXX gene amplification exhibited favorable responses to afatinib [62], underscoring the influence of molecular heterogeneity on afatinib efficacy in TNBC. As a monotherapy, afatinib showed limited activity in TNBC [63]. However, the combination of afatinib with dasatinib has shown promising clinical benefits in TNBC [64]. Additionally, combining afatinib with a palmitoylation inhibitor significantly suppressed tumor growth and metastasis in 4T1 tumor-bearing mice and prolonged survival [65]. These findings suggest that combining afatinib with other targeted therapies or chemotherapy may help overcome resistance and improve its therapeutic efficacy in TNBC.

This study has several limitations that may hinder direct recapitulation of human TNBC progression and complicate immediate clinical translation. Human TNBC is a highly heterogeneous disease comprising multiple molecular subtypes, including basal-like 1, basal-like 2, immunomodulatory, mesenchymal, mesenchymal stem-like, and luminal androgen receptor subtypes [2]. However, the present study was restricted to a limited number of cell lines representing the basal-like and mesenchymal-like subtypes only through each cell line. This narrow selection fails to capture the full spectrum of TNBC molecular and phenotypic diversity observed in patients. Our findings may not be generalizable across all TNBC subtypes. Future studies should expand the panel to include a broader repertoire of well-characterized TNBC cell lines that comprehensively represent all major subtypes. In addition, functional validation should be performed by comparing cytokine profiles, immune-related gene signatures, and microenvironmental interactions across these subtypes to better define subtype-specific behaviors and therapeutic vulnerabilities.

In conclusion, afatinib attenuates tumorigenic potentials of TNBC by inhibiting EGFR-mediated downstream signaling and EMT, reducing proinflammatory chemokine expression, and disrupting cell cycle progression, highlighting it as a promising therapeutic agent for TNBC. Combining afatinib with chemotherapeutic agents supports further preclinical evaluation to overcome resistance and enhance therapeutic efficacy in TNBC. Furthermore, afatinib-induced downregulation of proinflammatory chemokines may help support the efficacy of immunotherapy by favorably remodeling the tumor immune microenvironment when combined with immune-modulating agents.

Supplementary Materials: The following supporting information can be downloaded at: https://media.sciltp.com/articles/others/2605191515314416/JIIM-25120070-SM.pdf.

Author Contributions: D.-S.S.: Conceptualization, methodology, software, validation, formal analysis, investigation, resources, data curation, writing—original draft preparation, visualization, supervision, project administration, funding acquisition; T.J.M., R.M.I. and S.E.H.: Methodology, software, validation, formal analysis, investigation, data curation, visualization; E.-S.L. and S.E.A.: Validation, resources, writing—review and editing, funding acquisition. All authors have agreed to the published version of the manuscript.

Funding: This research was funded, either in whole or in part, by the National Institutes of Health (NIH) through the following grants: R25CA214220 (S.E.H.), R01ES031282 (E.-S.L.), SC1CA200519 (D.-S.S.), U54MD007586 (S.E.A.), U54CA163069 (D.-S.S., S.E.A.), and ACS DICRIDG-21-071-01-DICRIDG (D.-S.S., S.E.A.).

Institutional Review Board Statement: The study was conducted according to the NIH guide for the Care and Use of Laboratory Animals, and approved by the Institutional Animal Care and Use Committee at Meharry Medical College (eProtocol #16-03-511 and date of approval: 19 February 2016).

Informed Consent Statement: Not applicable.

Data Availability Statement: Not applicable.

Conflicts of Interest: The authors declare no conflicts of interest.

Use of AI and AI-Assisted Technologies: During the preparation of this work, the authors used Grok 4 free version to check grammatical correction. After using this tool, the authors reviewed and edited the content as needed and take full responsibility for the content of the published article. No AI tools were utilized in manipulating any data for this paper.

References

1. Dogra, A.K.; Prakash, A.; Gupta, S.; Gupta, M. Prognostic Significance and Molecular Classification of Triple Negative Breast Cancer: A Systematic Review. *Eur. J. Breast Health* **2025**, *21*, 101. https://doi.org/10.4274/ejbh.galenos.2025.2024-10-2.
2. Lehmann, B.D.; Bauer, J.A.; Chen, X.; Sanders, M.E.; Chakravarthy, A.B.; Shyr, Y.; Pietenpol, J.A. Identification of human triple-negative breast cancer subtypes and preclinical models for selection of targeted therapies. *J. Clin. Invest.* **2011**, *121*, 2750–2767. https://doi.org/10.1172/jci45014.
3. Ignacio, R.M.C.; Gibbs, C.R.; Lee, E.S.; Son, D.S. The TGFα-EGFR-Akt signaling axis plays a role in enhancing proinflammatory chemokines in triple-negative breast cancer cells. *Oncotarget* **2018**, *9*, 29286–29303. https://doi.org/10.18632/oncotarget.25389.
4. Son, D.S.; Kabir, S.M.; Dong, Y.; Lee, E.; Adunyah, S.E. Characteristics of chemokine signatures elicited by EGF and TNF in ovarian cancer cells. *J. Inflamm.* **2013**, *10*, 25. https://doi.org/10.1186/1476-9255-10-25.
5. Atwell, B.; Chalasani, P.; Schroeder, J. Nuclear epidermal growth factor receptor as a therapeutic target. *Explor Target Antitumor Ther* **2023**, *4*, 616–629. https://doi.org/10.37349/etat.2023.00156.
6. Gupta, G.K.; Collier, A.L.; Lee, D.; Hoefer, R.A.; Zheleva, V.; Siewertsz van Reesema, L.L.; Tang-Tan, A.M.; Guye, M.L.; Chang, D.Z.; Winston, J.S.; et al. Perspectives on Triple-Negative Breast Cancer: Current Treatment Strategies, Unmet Needs, and Potential Targets for Future Therapies. *Cancers* **2020**, *12*, 2392. https://doi.org/10.3390/cancers12092392.
7. Son, D.-S.; Obot, J.E.; Campbell, K.; Lee, E.-S.; Adunyah, S.E. Differential Effects of Afatinib on Cytokine-and Oncology-Related Profiles in Mesenchymal and Basal-Like 1 Triple-Negative Breast Cancer Cells. *J. Inflamm. Infect. Med.* **2025**, *1*, 1.
8. Sabit, H.; Adel, A.; Abdelfattah, M.M.; Ramadan, R.M.; Nazih, M.; Abdel-Ghany, S.; El-Hashash, A.; Arneth, B. The role of tumor microenvironment and immune cell crosstalk in triple-negative breast cancer (TNBC): Emerging therapeutic opportunities. *Cancer Lett.* **2025**, *628*, 217865. https://doi.org/10.1016/j.canlet.2025.217865.
9. Son, D.S.; Done, K.A.; Son, J.; Izban, M.G.; Virgous, C.; Lee, E.S.; Adunyah, S.E. Intermittent Fasting Attenuates Obesity-Induced Triple-Negative Breast Cancer Progression by Disrupting Cell Cycle, Epithelial-Mesenchymal Transition, Immune Contexture, and Proinflammatory Signature. *Nutrients* **2024**, *16*, 2101. https://doi.org/10.3390/nu16132101.
10. Gibby, K.; You, W.K.; Kadoya, K.; Helgadottir, H.; Young, L.J.; Ellies, L.G.; Chang, Y.; Cardiff, R.D.; Stallcup, W.B. Early vascular deficits are correlated with delayed mammary tumorigenesis in the MMTV-PyMT transgenic mouse following genetic ablation of the NG2 proteoglycan. *Breast Cancer Res.* **2012**, *14*, R67. https://doi.org/10.1186/bcr3174.
11. Ignacio, R.M.C.; Lee, E.S.; Wilson, A.J.; Beeghly-Fadiel, A.; Whalen, M.M.; Son, D.S. Obesity-Induced Peritoneal Dissemination of Ovarian Cancer and Dominant Recruitment of Macrophages in Ascites. *Immune Netw.* **2018**, *18*, e47. https://doi.org/10.4110/in.2018.18.e47.
12. Son, D.-S.; Ignacio, R.M.C.; Son, J.; Lee, E.-S.; Adunyah, S.E. Proinflammatory Effects of Obesity in the Progression of Triple Negative Breast Cancer. *J. Inflamm. Infect. Med.* **2025**, *1*, 2.
13. Dong, Y.L.; Kabir, S.M.; Lee, E.S.; Son, D.S. CXCR2-driven ovarian cancer progression involves upregulation of proinflammatory chemokines by potentiating NF-κB activation via EGFR-transactivated Akt signaling. *PLoS ONE* **2013**, *8*, e83789. https://doi.org/10.1371/journal.pone.0083789.
14. Romero-Moreno, R.; Curtis, K.J.; Coughlin, T.R.; Miranda-Vergara, M.C.; Dutta, S.; Natarajan, A.; Facchine, B.A.; Jackson, K.M.; Nystrom, L.; Li, J.; et al. The CXCL5/CXCR2 axis is sufficient to promote breast cancer colonization during bone metastasis. *Nat. Commun.* **2019**, *10*, 4404. https://doi.org/10.1038/s41467-019-12108-6.
15. Xu, J.; Zhang, W.; Tang, L.; Chen, W.; Guan, X. Epithelial-mesenchymal transition induced PAI-1 is associated with prognosis of triple-negative breast cancer patients. *Gene* **2018**, *670*, 7–14. https://doi.org/10.1016/j.gene.2018.05.089.
16. Sureshbabu, A.; Okajima, H.; Yamanaka, D.; Tonner, E.; Shastri, S.; Maycock, J.; Szymanowska, M.; Shand, J.; Takahashi, S.; Beattie, J.; et al. IGFBP5 induces cell adhesion, increases cell survival and inhibits cell migration in MCF-7 human breast cancer cells. *J. Cell Sci.* **2012**, *125*, 1693–1705. https://doi.org/10.1242/jcs.092882.
17. Rodríguez-Rojas, K.; Cortes-Reynosa, P.; Torres-Alamilla, P.; Rodríguez-Ochoa, N.; Salazar, E.P. A novel role of IGFBP5 in the migration, invasion and spheroids formation induced by IGF-I and insulin in MCF-7 breast cancer cells. *Breast Cancer Res. Treat.* **2024**, *208*, 79–88. https://doi.org/10.1007/s10549-024-07397-5.
18. Dittmer, J. Biological effects and regulation of IGFBP5 in breast cancer. *Front. Endocrinol.* **2022**, *13*, 983793. https://doi.org/10.3389/fendo.2022.983793.
19. Cretu, A.; Sha, X.; Tront, J.; Hoffman, B.; Liebermann, D.A. Stress sensor Gadd45 genes as therapeutic targets in cancer. *Cancer Ther.* **2009**, *7*, 268–276.

20. Adinew, G.M.; Messeha, S.S.; Taka, E.; Badisa, R.B.; Antonie, L.M.; Soliman, K.F.A. Thymoquinone Alterations of the Apoptotic Gene Expressions and Cell Cycle Arrest in Genetically Distinct Triple-Negative Breast Cancer Cells. *Nutrients* **2022**, *14*, 2120. https://doi.org/10.3390/nu14102120.
21. Goodarzi, A.A.; Block, W.D.; Lees-Miller, S.P. The role of ATM and ATR in DNA damage-induced cell cycle control. *Prog. Cell Cycle Res.* **2003**, *5*, 393–411.
22. Sofianidi, A.; Dumbrava, E.E.; Syrigos, K.N.; Nasrazadani, A. Triple-Negative Breast Cancer and Emerging Therapeutic Strategies: ATR and CHK1/2 as Promising Targets. *Cancers* **2024**, *16*, 1139. https://doi.org/10.3390/cancers16061139.
23. Hu, Y.M.; Liu, X.C.; Hu, L.; Dong, Z.W.; Yao, H.Y.; Wang, Y.J.; Zhao, W.J.; Xiang, Y.K.; Liu, Y.; Wang, H.B.; et al. Inhibition of the ATR-DNAPKcs-RB axis drives G1/S-phase transition and sensitizes triple-negative breast cancer (TNBC) to DNA holliday junctions. *Biochem. Pharmacol.* **2024**, *225*, 116310. https://doi.org/10.1016/j.bcp.2024.116310.
24. Knudsen, E.S.; Pruitt, S.C.; Hershberger, P.A.; Witkiewicz, A.K.; Goodrich, D.W. Cell Cycle and Beyond: Exploiting New RB1 Controlled Mechanisms for Cancer Therapy. *Trends Cancer* **2019**, *5*, 308–324. https://doi.org/10.1016/j.trecan.2019.03.005.
25. Robinson, T.J.; Liu, J.C.; Vizeacoumar, F.; Sun, T.; Maclean, N.; Egan, S.E.; Schimmer, A.D.; Datti, A.; Zacksenhaus, E. RB1 status in triple negative breast cancer cells dictates response to radiation treatment and selective therapeutic drugs. *PLoS ONE* **2013**, *8*, e78641. https://doi.org/10.1371/journal.pone.0078641.
26. Jauhiainen, A.; Thomsen, C.; Strömbom, L.; Grundevik, P.; Andersson, C.; Danielsson, A.; Andersson, M.K.; Nerman, O.; Rörkvist, L.; Ståhlberg, A.; et al. Distinct cytoplasmic and nuclear functions of the stress induced protein DDIT3/CHOP/GADD153. *PLoS ONE* **2012**, *7*, e33208. https://doi.org/10.1371/journal.pone.0033208.
27. Zhu, S.L.; Qi, M.; Chen, M.T.; Lin, J.P.; Huang, H.F.; Deng, L.J.; Zhou, X.W. A novel DDIT3 activator dehydroevodiamine effectively inhibits tumor growth and tumor cell stemness in pancreatic cancer. *Phytomedicine* **2024**, *128*, 155377. https://doi.org/10.1016/j.phymed.2024.155377.
28. Block, I.; Müller, C.; Sdogati, D.; Pedersen, H.; List, M.; Jaskot, A.M.; Syse, S.D.; Lund Hansen, P.; Schmidt, S.; Christiansen, H.; et al. CFP suppresses breast cancer cell growth by TES-mediated upregulation of the transcription factor DDIT3. *Oncogene* **2019**, *38*, 4560–4573. https://doi.org/10.1038/s41388-019-0739-0.
29. Sancho, S.; Young, P.; Suter, U. Regulation of Schwann cell proliferation and apoptosis in PMP22-deficient mice and mouse models of Charcot-Marie-Tooth disease type 1A. *Brain* **2001**, *124*, 2177–2187. https://doi.org/10.1093/brain/124.11.2177.
30. Winslow, S.; Leandersson, K.; Larsson, C. Regulation of PMP22 mRNA by G3BP1 affects cell proliferation in breast cancer cells. *Mol. Cancer* **2013**, *12*, 156. https://doi.org/10.1186/1476-4598-12-156.
31. Polyak, K.; Kato, J.Y.; Solomon, M.J.; Sherr, C.J.; Massague, J.; Roberts, J.M.; Koff, A. p27Kip1, a cyclin-Cdk inhibitor, links transforming growth factor-beta and contact inhibition to cell cycle arrest. *Genes Dev.* **1994**, *8*, 9–22. https://doi.org/10.1101/gad.8.1.9.
32. Wang, H.; Yang, T.; Yuan, Y.; Sun, X. Identification of FOXE3 transcription factor as a potent oncogenic factor in triple-negative breast cancer. *Biochem. Biophys. Res. Commun.* **2020**, *523*, 78–85. https://doi.org/10.1016/j.bbrc.2019.12.034.
33. Ma, H.; Dong, Y.; Zheng, J.; Zhang, S.; Tang, S.; Wang, J.; Qu, Z.; Li, X.; Zeng, L.; Song, K.; et al. CDKN3 as a key regulator of G2M phase in triple-negative breast cancer: Insights from multi-transcriptomic analysis. *IUBMB Life* **2025**, *77*, e2922. https://doi.org/10.1002/iub.2922.
34. Liu, Y.; Zhang, A.; Bao, P.P.; Lin, L.; Wang, Y.; Wu, H.; Shu, X.O.; Liu, A.; Cai, Q. MicroRNA-374b inhibits breast cancer progression through regulating CCND1 and TGFA genes. *Carcinogenesis* **2021**, *42*, 528–536. https://doi.org/10.1093/carcin/bgab005.
35. Yuan, C.; Wang, C.; Wang, J.; Kumar, V.; Anwar, F.; Xiao, F.; Mushtaq, G.; Liu, Y.; Kamal, M.A.; Yuan, D. Inhibition on the growth of human MDA-MB-231 breast cancer cells *in vitro* and tumor growth in a mouse xenograft model by Se-containing polysaccharides from Pyracantha fortuneana. *Nutr. Res.* **2016**, *36*, 1243–1254. https://doi.org/10.1016/j.nutres.2016.09.012.
36. Uxa, S.; Castillo-Binder, P.; Kohler, R.; Stangner, K.; Müller, G.A.; Engeland, K. Ki-67 gene expression. *Cell Death Differ.* **2021**, *28*, 3357–3370. https://doi.org/10.1038/s41418-021-00823-x.
37. Song, C.; Lowe, V.J.; Lee, S. Inhibition of Cdc20 suppresses the metastasis in triple negative breast cancer (TNBC). *Breast Cancer* **2021**, *28*, 1073–1086. https://doi.org/10.1007/s12282-021-01242-z.
38. Aljohani, A.I.; Toss, M.S.; Green, A.R.; Rakha, E.A. The clinical significance of cyclin B1 (CCNB1) in invasive breast cancer with emphasis on its contribution to lymphovascular invasion development. *Breast Cancer Res. Treat.* **2023**, *198*, 423–435. https://doi.org/10.1007/s10549-022-06801-2.
39. Li, M.X.; Jin, L.T.; Wang, T.J.; Feng, Y.J.; Pan, C.P.; Zhao, D.M.; Shao, J. Identification of potential core genes in triple negative breast cancer using bioinformatics analysis. *Onco Targets Ther.* **2018**, *11*, 4105–4112. https://doi.org/10.2147/ott.S166567.

40. Zhang, S.; Tischer, T.; Barford, D. Cyclin A2 degradation during the spindle assembly checkpoint requires multiple binding modes to the APC/C. *Nat. Commun.* **2019**, *10*, 3863. https://doi.org/10.1038/s41467-019-11833-2.
41. Lu, Y.; Yang, G.; Xiao, Y.; Zhang, T.; Su, F.; Chang, R.; Ling, X.; Bai, Y. Upregulated cyclins may be novel genes for triple-negative breast cancer based on bioinformatic analysis. *Breast Cancer* **2020**, *27*, 903–911. https://doi.org/10.1007/s12282-020-01086-z.
42. Adinew, G.M.; Messeha, S.; Taka, E.; Soliman, K.F.A. The Prognostic and Therapeutic Implications of the Chemoresistance Gene BIRC5 in Triple-Negative Breast Cancer. *Cancers* **2022**, *14*, 5180. https://doi.org/10.3390/cancers14215180.
43. Wang, C.; Zheng, X.; Shen, C.; Shi, Y. MicroRNA-203 suppresses cell proliferation and migration by targeting BIRC5 and LASP1 in human triple-negative breast cancer cells. *J. Exp. Clin. Cancer Res.* **2012**, *31*, 58. https://doi.org/10.1186/1756-9966-31-58.
44. Lu, Z.; Wang, Z.; Li, G. High expression of CCNB2 is an independent predictive poor prognostic biomarker and correlates with immune infiltrates in breast carcinoma. *Heliyon* **2024**, *10*, e31586. https://doi.org/10.1016/j.heliyon.2024.e31586.
45. Wu, S.; Su, R.; Jia, H. Cyclin B2 (CCNB2) Stimulates the Proliferation of Triple-Negative Breast Cancer (TNBC) Cells *in Vitro* and *in Vivo*. *Dis. Markers* **2021**, *2021*, 5511041. https://doi.org/10.1155/2021/5511041.
46. Cao, J.; Sun, S.; Min, R.; Li, R.; Fan, X.; Han, Y.; Feng, Z.; Li, N. Prognostic Significance of CCNB2 Expression in Triple-Negative Breast Cancer. *Cancer Manag. Res* **2021**, *13*, 9477–9487. https://doi.org/10.2147/cmar.S339105.
47. Kreis, N.N.; Louwen, F.; Yuan, J. The Multifaceted p21 (Cip1/Waf1/CDKN1A) in Cell Differentiation, Migration and Cancer Therapy. *Cancers* **2019**, *11*, 1220. https://doi.org/10.3390/cancers11091220.
48. Vats, P.; Saini, C.; Baweja, B.; Srivastava, S.K.; Kumar, A.; Kushwah, A.S.; Nema, R. Aurora kinases signaling in cancer: From molecular perception to targeted therapies. *Mol. Cancer* **2025**, *24*, 180. https://doi.org/10.1186/s12943-025-02353-3.
49. Ning, B.; Liu, C.; Kucukdagli, A.C.; Zhang, J.; Jing, H.; Zhou, Z.; Zhang, Y.; Dong, Y.; Chen, Y.; Guo, H.; et al. Proteomic profiling identifies upregulation of aurora kinases causing resistance to taxane-type chemotherapy in triple negative breast cancer. *Sci. Rep.* **2025**, *15*, 3211. https://doi.org/10.1038/s41598-025-87315-x.
50. Kozyreva, V.K.; Kiseleva, A.A.; Ice, R.J.; Jones, B.C.; Loskutov, Y.V.; Matalkah, F.; Smolkin, M.B.; Marinak, K.; Livengood, R.H.; Salkeni, M.A.; et al. Combination of Eribulin and Aurora A Inhibitor MLN8237 Prevents Metastatic Colonization and Induces Cytotoxic Autophagy in Breast Cancer. *Mol. Cancer Ther.* **2016**, *15*, 1809–1822. https://doi.org/10.1158/1535-7163.Mct-15-0688.
51. Pellizzari, S.; Athwal, H.; Bonvissuto, A.C.; Parsyan, A. Role of AURKB Inhibition in Reducing Proliferation and Enhancing Effects of Radiotherapy in Triple-Negative Breast Cancer. *Breast Cancer* **2024**, *16*, 341–346. https://doi.org/10.2147/bctt.S444965.
52. Borlado, L.R.; Méndez, J. CDC6: From DNA replication to cell cycle checkpoints and oncogenesis. *Carcinogenesis* **2007**, *29*, 237–243. https://doi.org/10.1093/carcin/bgm268.
53. Li, C.; Zhang, E.D.; Yu, R.; Yuan, B.; Yang, Y.; Zeng, Z.; Huang, H. Comprehensive multi-omics analysis showed that CDC6 is a potential prognostic and immunotherapy biomarker for multiple cancer types including HCC. *Transl. Oncol.* **2025**, *53*, 102314. https://doi.org/10.1016/j.tranon.2025.102314.
54. Mahadevappa, R.; Neves, H.; Yuen, S.M.; Bai, Y.; McCrudden, C.M.; Yuen, H.F.; Wen, Q.; Zhang, S.D.; Kwok, H.F. The prognostic significance of Cdc6 and Cdt1 in breast cancer. *Sci. Rep.* **2017**, *7*, 985. https://doi.org/10.1038/s41598-017-00998-9.
55. Fang, Y.; Zhang, X. Targeting NEK2 as a promising therapeutic approach for cancer treatment. *Cell Cycle* **2016**, *15*, 895–907. https://doi.org/10.1080/15384101.2016.1152430.
56. Naro, C.; Barbagallo, F.; Caggiano, C.; De Musso, M.; Panzeri, V.; Di Agostino, S.; Paronetto, M.P.; Sette, C. Functional Interaction Between the Oncogenic Kinase NEK2 and Sam68 Promotes a Splicing Program Involved in Migration and Invasion in Triple-Negative Breast Cancer. *Front. Oncol.* **2022**, *12*, 880654. https://doi.org/10.3389/fonc.2022.880654.
57. Naro, C.; De Musso, M.; Delle Monache, F.; Panzeri, V.; de la Grange, P.; Sette, C. The oncogenic kinase NEK2 regulates an RBFOX2-dependent pro-mesenchymal splicing program in triple-negative breast cancer cells. *J. Exp. Clin. Cancer Res.* **2021**, *40*, 397. https://doi.org/10.1186/s13046-021-02210-3.
58. Deeks, E.D.; Keating, G.M. Afatinib in advanced NSCLC: A profile of its use. *Drugs Ther. Perspect.* **2018**, *34*, 89–98. https://doi.org/10.1007/s40267-018-0482-6.
59. Keating, G.M. Afatinib: A Review in Advanced Non-Small Cell Lung Cancer. *Target. Oncol.* **2016**, *11*, 825–835. https://doi.org/10.1007/s11523-016-0465-2.
60. Nakai, K.; Hung, M.C.; Yamaguchi, H. A perspective on anti-EGFR therapies targeting triple-negative breast cancer. *Am. J. Cancer Res.* **2016**, *6*, 1609–1623.

61. Pellecchia, S.; Franchini, M.; Viscido, G.; Arnese, R.; Gambardella, G. Single cell lineage tracing reveals clonal dynamics of anti-EGFR therapy resistance in triple negative breast cancer. *Genome Med.* **2024**, *16*, 55. https://doi.org/10.1186/s13073-024-01327-2.
62. Lin, P.H.; Tseng, L.M.; Lee, Y.H.; Chen, S.T.; Yeh, D.C.; Dai, M.S.; Liu, L.C.; Wang, M.Y.; Lo, C.; Chang, S.; et al. Neoadjuvant afatinib with paclitaxel for triple-negative breast cancer and the molecular characteristics in responders and non-responders. *J. Formos. Med. Assoc.* **2022**, *121*, 2538–2547. https://doi.org/10.1016/j.jfma.2022.05.015.
63. Schuler, M.; Awada, A.; Harter, P.; Canon, J.L.; Possinger, K.; Schmidt, M.; De Grève, J.; Neven, P.; Dirix, L.; Jonat, W.; et al. A phase II trial to assess efficacy and safety of afatinib in extensively pretreated patients with HER2-negative metastatic breast cancer. *Breast Cancer Res. Treat.* **2012**, *134*, 1149–1159. https://doi.org/10.1007/s10549-012-2126-1.
64. Canonici, A.; Browne, A.L.; Ibrahim, M.F.K.; Fanning, K.P.; Roche, S.; Conlon, N.T.; O'Neill, F.; Meiller, J.; Cremona, M.; Morgan, C.; et al. Combined targeting EGFR and SRC as a potential novel therapeutic approach for the treatment of triple negative breast cancer. *Ther. Adv. Med. Oncol.* **2020**, *12*, 1758835919897546. https://doi.org/10.1177/1758835919897546.
65. Wang, X.; Zhu, X.; Li, B.; Wei, X.; Chen, Y.; Zhang, Y.; Wang, Y.; Zhang, W.; Liu, S.; Liu, Z.; et al. Intelligent Biomimetic Nanoplatform for Systemic Treatment of Metastatic Triple-Negative Breast Cancer via Enhanced EGFR-Targeted Therapy and Immunotherapy. *ACS Appl. Mater. Interfaces* **2022**, *14*, 23152–23163. https://doi.org/10.1021/acsami.2c02925.